N87-22217

NON-LINEAR PERFORMANCE OF A THREE-BEARING ROTOR

INCORPORATING A SQUEEZE-FILM DAMPER

R. Holmes and M. Dede
University of Southampton
Southampton, England

This paper is concerned with the non-linear vibration performance of a rigid rotor supported on three bearings, one being surrounded by a squeeze-film damper. This damper relies on the pressure built up in the squeeze film to help counter-act external forces arising from unbalance and other effects. As a result a vibration orbit of a certain magnitude results.

Such vibration orbits illustrate features found in other non-linear systems, in particular sub-harmonic resonances and jump phenomena. Comparisons between theoretical predictions and experimental observations of these phenomena are made.

INTRODUCTION

The rotors of aero-engine gas turbines are often supported on three rolling-element bearings, the intermediate bearing usually providing a thrust capacity. The reason for this is that axial expansions take place from the thrust face and, being proportional to distances along the shaft to the ends of the rotor, these expansions do not impose such stringent demands on axial clearance at these ends as they would if the thrust bearing were at one extreme end of the rotor.

However, many aero-engine rotors are stiff, (running well below any flexural critical speed), and this means that problems of misalignment almost inevitably exist. The presence of a squeeze-film damper around one of the bearings helps considerably to alleviate these problems. However, since such dampers carry very little radial load under these circumstances, non-linear response to unbalance and sub-harmonic resonance with the casing flexibility are likely to occur.

Non-linear response manifests itself as persistence of synchronous vibration well beyond the undamped natural frequency of the assembly with a sudden jump-down to a lower vibration level at some higher speed. During engine run-down the lower vibration level persists until a speed lower than the original jump-down speed is reached, when a sudden jump-up will occur in the vibration amplitude. On occasion a jump-up with run-up has also been observed.

Sub-harmonic resonances occur due to the weak non-linearity offered by the squeeze-film damper, usually at rotational speeds equal to some integer multiple of the natural frequency of either of the bounce modes of the rigid rotor in its casing. These resonances can be just as damaging in their own way as the resonances which occur at speeds equal to these natural frequencies (that is when the integer is unity).

A	$\pi\eta R(\ell/c)^3/\sqrt{km}$
c	radial clearance of squeeze film
C_J	dynamic journal (or rotor) centre
C_{JS}	equilibrium position of journal centre
C_B	centre of oil container (bearing)
e	eccentricity of journal in bearing
F	dynamic force transmitted to engine frame
k	stiffness of parallel spring per land
$\overline{K}$	$k/m\omega^2$
ℓ	squeeze-film land length
m	journal mass per land
P_1, P_2	squeeze-film forces
P_c	rotating force vector per land
Q_c	$P_c/mc\omega^2 = u/c$
R	journal radius
T	transmissibility
t	time
u	displacement of rotor centre of mass from geometric centre due to addition of unbalance mass or loss of mass.
β	$\eta R\ell^3/mc^3\omega$
ϵ	dynamic eccentricity ratio (= e/c)
η	oil viscosity
ψ	dynamic attitude angle
ω	frequency of dynamic load
ω_n	$\sqrt{k/m}$
λ	$\eta\ell R^3/mc^2$
w_j	journal angular velocity
f, F, $h_{1,2}$	functions of

FEATURES OF THE PRESENT INVESTIGATION

To elucidate these problems, consider a stiff rotor in its flexible casing (Fig. 1a), in which the intermediate bearing is surrounded by a squeeze-film damper. To formulate ideas let the stiffnesses of bearing pedestals 1 and 2 be high compared with that of bearing 3. Further, assume that bearing 2 is held fairly centrally within its squeeze-film damper. Under these circumstances the equivalent system can be drawn as in Fig. 1b, in which m, k and b are equivalent properties decided by the dimensions of the original assembly. In particular, b will describe a non-linear damper.

During running any vibration is likely to produce a concentric orbit and the squeeze-film damper is not called upon to provide a static load-carrying capacity. Consequently, if the oil-supply pressure is of reasonable magnitude, the damper annulus remains full. The damper is often supplied with oil to a central circumferential oil groove which effectively separates the squeeze film axially into two parts or lands. Governing parameters are usually assumed to be appropriate to one land.

If the oil supply to the damper is sufficient for the squeeze-film to remain full and uncavitated a rotor vibration response curve such as (a) in Fig. 2 may be expected [1], [2]. If however cavitation occurs, this has the effect of introducing a stiffness term in the radial restoring force provided by the squeeze film and curves such as (b) are predicted [1]. The latter curve reveals a hardening-stiffness non-linearity and a deleterious influence on rotor response. At moderate frequencies three amplitude ratios are possible, the intermediate ratio being unstable, resulting in a jump-down with engine run-up and a jump-up with engine run-down. Such jumps have been reported in practical systems, as has the occasional jump-up with increase in engine speed. Fig. 2c shows the result of accelerating a rotor up to a speed of 3500 rev/min. and back over a period of 8.3 minutes. The degree of blackness depicts the strength of each harmonic from 1 x rotor speed to 3 x rotor speed, the other harmonics being practically non-existent. A predominant feature is the disappearance of the 2 x and 3 x harmonics after the jump-down on run-up and a reappearance of them after the jump-up on run-down. This suggests that the jumps form a demarcation between effectively linear and non-linear vibration and have been noted in test engines. Numerical investigations have also been carried out to test the possibility of sub-harmonic resonance arising [1]. Fig. 3 shows predicted sub-harmonic transients for a rotor-bearing assembly incorporating a squeeze-film offering fairly light damping. Subharmonic vibration occurs at speeds in the regions of two, three and four times the lower bounce mode critical speed. Such effects have also been reported in practical systems [3].

Very few experimental programs have been conducted to investigate problems of non-linear jumps and subharmonic resonances in rotor-bearing assemblies. The experiments of Nikolajsen et al [3] and Simandiri et al [4] are limited respectively to flexible transmission shafts with squeeze-film isolators and to a highly idealised test facility, showing little resemblance to an engine assembly.

RESPONSE CALCULATIONS

Fig. 4 shows in diagrammatic form the outer race of a rolling-element bearing within the oil container (the bearing pedestal), under the action of a restoring force $kc\epsilon$ arising from the equivalent stiffness k of a parallel spring as in Fig. 1b. Vibration results from a dynamic force P_c due to some cause, such as unbalance. The amplitude of orbital motion depends upon $kc\epsilon$, P_c, P_1 and P_2, the

351

last two forces arising hydrodynamically from the squeeze-film. Any gravity load on the squeeze-film is assumed to be effectively neutralised by the parallel spring.

The equations governing the concentric motion of the shaft centre are then,

$$P_c \cos(\omega t - \psi) - P_1 - kc\epsilon = -mc\epsilon\omega^2$$

and
$$\qquad \dots (1)$$

$$P_c \sin(\omega t - \psi) - P_2 = 0$$

where ϵ is the dynamic eccentricity ratio resulting from unbalance. In equations (1) the squeeze-film forces, P_1 and P_2, can be shown from hydrodynamic considerations, to be given, for concentric motion, by

and
$$P_1 = 0$$

$$P_2 = \frac{\pi\eta R\ell^3}{c^2(1 - \epsilon^2)^{3/2}} \cdot \epsilon\omega \qquad \dots (2)$$

Equations (1) may be made non-dimensional by dividing by $mc\omega^2$ to give

$$Q_c \cos(\omega t - \psi) = -\epsilon(1 - \bar{K})$$

and
$$\qquad \dots (3)$$

$$Q_c \sin(\omega t - \psi) = \frac{\pi\eta R}{m\omega} \left(\frac{\ell}{c}\right)^3 \cdot \frac{\epsilon}{(1 - \epsilon^2)^{3/2}}$$

where $\bar{K} = k/m\omega^2 = (\omega/\omega_n)^{-2}$, and $Q_c = P_c/mc\omega^2$.

If P_c arises due to mass unbalance mu, then $P_c = mu\omega^2$ and $Q_c = u/c$.

Putting $\beta = \frac{\eta R(\ell/c)^3}{m\omega}$, equations (3) may be re-written to give

$$\frac{u}{c} \cos(\omega t - \psi) = (\bar{K} - 1)\epsilon$$

and
$$\qquad \dots (4)$$

$$\frac{u}{c} \sin(\omega t - \psi) = \pi\beta\epsilon/(1 - \epsilon^2)^{3/2}$$

Hence, after some manipulation, we obtain

$$\cdot \left[\frac{u}{c}\right]^2 \frac{(1 - \epsilon^2)^3}{\epsilon^2} \cdot \left[\frac{\omega}{\omega_n}\right]^4 = A^2 \left[\frac{\omega}{\omega_n}\right]^2 + [1 - \left[\frac{\omega}{\omega_n}\right]^2]^2 (1 - \epsilon^2)^3 \qquad \dots (5)$$

where
$$A = \frac{\pi\eta R}{\sqrt{km}} \left(\frac{\ell}{c}\right)^3$$

and
$$\omega_n = \sqrt{k/m}$$

Assuming a fairly typical value of $A = 0.0^7$, say, a family of response curves of $\frac{\epsilon}{u/c}$ versus ω/ω_n may be constructed for different values of u/c (Fig.5a).
From these curves an indication can be obtained of the amount of vibration ϵ, suffered by the rotor in the symmetric bounce mode, a common mode of vibration in many rotating assemblies. Of equal importance is the dynamic force F transmitted to the engine frame. Bearing in mind that P_1 is zero, the force F is given by

$$F = [P_2{}^2 + (kc\epsilon)^2]^{1/2} \qquad \dots (6)$$

and is best expressed as a ratio (the transmissibility) of the unbalance force P_c. This transmissibility T is given by

$$T = F/P_c = \frac{F/mc\omega^2}{u/c} \qquad \ldots (7)$$

From equations (2), (6) and (7) we obtain

$$T^2 = \left[\frac{\pi^2\beta^2\epsilon^2}{(1-\epsilon^2)^3} + \bar{k}^2\epsilon^2 \right] / (u/c)^2$$

Now from equation (4),

$$\frac{\pi^2\beta^2\epsilon^2}{(1-\epsilon^2)^3} = (u/c)^2 - \epsilon^2 [\bar{k}-1]^2$$

and so finally

$$T^2 = 1 + \left(\frac{\epsilon}{u/c}\right)^2 \left[\frac{2}{(\omega/\omega_n)^2} - 1\right]$$

Again, assuming a value of A of 0.07, a family of curves showing the dependence of T on ω/ω_n for different values of u/c is shown in Fig. 5b.

An inspection of Figs. 5a and 5b shows that both $\epsilon/(u/c)$ and the transmissibility T depend upon u/c. This is expected since the system is essentially non-linear. Also, only for ω/ω_n above $\sqrt{2}$, is T less than unity. This speed ratio should thus be made to correspond to the lower limit of normal operation of the engine, when it can readily be seen from Figs 3a and 3b that a low value of u/c is desirable on three counts - low vibration amplitude, low transmissibility and low transmitted force.

Now suppose that the supply pressure is insufficient to maintain a positive pressure in areas of the squeeze film where the boundary surfaces are instantaneously separating. For the sake of simplicity assume that as a result the squeeze film becomes half cavitated. It may then be shown that P_2 is halved and that P_1 is no longer zero, being given by

$$P_1 = \frac{2\eta R l^3 \omega}{c^2} \cdot \frac{\epsilon^2}{(1-\epsilon^2)^2}$$

Hence, for circular concentric whirl, we have the following equations which correspond to equations (4) for the uncavitated case

$$\frac{u}{c} \cos(\omega t - \psi) = (\bar{k}-1)\epsilon + \frac{2\beta\epsilon^2}{(1-\epsilon^2)^2}$$

$$\qquad \ldots (8)$$

$$\frac{u}{c} \sin(\omega t - \psi) = \frac{\pi\beta}{2} \cdot \frac{\epsilon}{(1-\epsilon^2)^{3/2}}$$

in which $\beta = A(\bar{k})^{\frac{1}{2}}/\pi$.

Hence $\left(\frac{u}{c}\right)^2 = \beta^2 \left[\frac{\pi^2\epsilon^2}{4(1-\epsilon^2)^3} + \frac{4\epsilon^4}{(1-\epsilon^2)^4} \right] + \epsilon^2(\bar{k}-1)^2$

$$+ \frac{4\epsilon^3}{(1-\epsilon^2)^2} \beta(\bar{k}-1) \qquad \ldots (9)$$

In this case

$$T^2 = \frac{\epsilon^2}{(u/c)^2} \left[\beta^2\left(\frac{\pi^2}{4(1-\epsilon^2)^3} + \frac{4\epsilon^2}{(1-\epsilon^2)^4}\right) + \bar{k}^2 + \frac{4\beta\epsilon\bar{k}}{(1-\epsilon^2)^2} \right]$$

Using equation (9) this may be rewritten as

$$T^2 = 1 + (\frac{\epsilon}{u/c})^2 \; [\frac{4\epsilon\beta}{(1-\epsilon^2)^2} + 2\bar{K} - 1]$$

in which $\bar{K} = k/m\omega^2 = (\frac{\omega}{\omega_n})^{-2}$

The effect of cavitation is shown in Figs. 5c, d, which reveal a deleterious influence on vibration and on transmissibility. The distortions in the response curves of Fig. 5c compared with what one would expect from a linear system are responsible for the so-called jump phenomenon. At high frequencies three amplitude ratios are possible, the intermediate one being unstable.

STABILITY CONSIDERATIONS

In most applications of a journal bearing we are concerned with the stability of a static equilibrium position e.g. [6]. In the present work it is necessary to consider the stability of a circular concentric equilibrium orbit. The two cases can be compared as shown in Fig. 6a, b. It may be shown [6] that for perturbations from a static equilibrium position the hydrodynamic forces P_1' and P_2' of a journal bearing oil film are given by

$$P_{1,2}' = \lambda\omega_j(1 - 2\dot{\alpha}/\omega_j)f_{1,2}(\epsilon, \frac{\dot{\epsilon}/\omega_j}{1 - 2\dot{\alpha}/\omega_j})$$

With little loss of accuracy [7] we may write them as

$$P_1' = \dot{\epsilon}F_1(\epsilon) \pm (\frac{\omega_j}{2} - \dot{\alpha}) h_1(\epsilon)$$

$$P_2' = \dot{\epsilon}F_2(\epsilon) \pm (\frac{\omega_j}{2} - \dot{\alpha}) h_2(\epsilon)$$

in which the positive sign relates to the squeeze damper and its force directions (Fig. 6b) and the negative sign to the journal bearing and its force directions (Fig. 6a). Now in the case of the squeeze damper, if the journal centre is moving on a circular concentric orbit at angular velocity $\dot{\alpha}_s$, then $\omega_j = 0$ and $\dot{\alpha} = \omega + \dot{\alpha}_s$.

Hence we finally have for the journal bearing

$$P_1' = \dot{\epsilon}F_1(\epsilon) - (\frac{\omega_j}{2} - \dot{\alpha}) h_1(\epsilon)$$

$$P_2' = \dot{\epsilon}F_2(\epsilon) - (\frac{\omega_j}{2} - \dot{\alpha}) h_2(\epsilon)$$

while for the squeeze-film damper

$$P_1' = \dot{\epsilon}F_1(\epsilon) - (\dot{\alpha}_s + \omega) h_1(\epsilon)$$
$$P_2' = \dot{\epsilon}F_2(\epsilon) - (\dot{\alpha}_s + \omega)h_2(\epsilon)$$

Now for a journal bearing, for $\dot{\alpha} \ll \omega_j$ and neglecting second order terms

$$dP_r = dP_1' - P_2'd\alpha = F_1 d\dot{\epsilon} - \frac{\omega_j}{2} \frac{\partial h_1}{\partial\epsilon} d\epsilon + h_1 d\dot{\alpha} + \frac{\omega_j}{2} h_2 d\alpha$$

and

$$dP_s = dP_2' + P_1'd\alpha = F_2 d\dot{\epsilon} - \frac{\omega_j}{2} \frac{\partial h_2}{\partial\epsilon} d\epsilon + h_2 d\dot{\alpha} - \frac{\omega_j}{2} h_1 d\alpha$$

while for a squeeze damper, for $\dot{\alpha}_s \ll \omega$

$$dP_r = dP_1' + P_2'd\alpha_s = F_1 d\dot{\epsilon} \quad - \omega \frac{\partial h_1}{\partial \epsilon} d\epsilon - h_1 d\dot{\alpha}_s \quad - \omega h_2\, d\alpha_s$$

$$dP_s = -dP_2' + P_1'\, d\alpha_s = -F_2 d\dot{\epsilon} \quad + \omega\frac{\partial h_2}{\partial \epsilon}\, d\epsilon + h_2\, d\dot{\alpha}_s - \omega h_1\, d\alpha_s$$

$$\ldots (10)$$

Now r, s correspond to the ϵ and α directions, respectively. Thus for the squeeze damper the direct damping terms are equal and of the same sign as for the journal bearing; the cross damping terms are equal but of opposite sign; the direct stiffness terms are twice the values and of the same sign, and the cross stiffness terms are twice the values and of opposite sign.

The effect of adding an extra radial force $kc\epsilon$ due to the retainer spring is to increase dP_r and dP_s respectively in equations (10) by $kcd\epsilon$ and $kc\,\epsilon d\alpha_s$. This in turn has the effect of adding the stiffness k to each of the direct stiffness terms in equations (10). Applying these new equations to perturbations of a rotor from a concentric circular orbit indicates that part of the response curve is indeed unstable.

SUBHARMONIC RESONANCE

Figure 3 shows subharmonic transients, which could persist if some negative damping were present to counteract the positive damping from the squeeze film damper. Such negative damping could emanate from any journal bearings present [3] or from internal shaft friction, say.

TEST RESULTS

To create a realistic engine configuration, a two-bearing test facility used in a previous research programme [5] has been adapted to form a three-bearing rigid rotor incorporating the essential features of a medium-sized aero-engine assembly. It is not uncommon in gas turbine rotor vibration for an antisymmetric rigid-rotor mode to exhibit a node near one of the rolling-element bearings. With such an application in mind, the test rig shown in Fig. 7 was used for the investigation of the squeeze-film damper, 1, at one of its three rolling-elements, 2. The self-aligning bearing, 3, constituted a pivot about which an antisymmetric (i.e. conical) mode of vibration would occur, when the rotor, 4, was acted upon by a force arising from rotation of the unbalance mass, 5. Flexible bars, 6, simulated the pedestal flexibility of an actual engine. The flexible bars were screwed into a heavy foundation block, 8, which represented ground. The squeeze-film dimensions sere set by the outer diameter of the rolling bearing (136 mm), and damper land (9 mm) and its radial clearance (0.216 mm). Oil of 6 cp viscosity was supplied to the damper via three supply holes, 9, and a central circumferential groove. End plates were attached at the ends of the outer element of the damper to afford some sealing. Proximity vibration pick-ups were used to measure the vibration of the shaft relative to the pedestal and relative to ground, and strain gauges were provided on the flexible bars from which transmitted forces were recorded.

Tests indicated the existence of jump phenomena during run-up and run-down, when the squeeze-film damper ran at low supply pressure (Fig. 8a), but no such jumps when it can with a higher supply pressure (Fig. 8b). These results agree with the trends predicted by Figs. 2b and 2a and by Fig 5c, d.

355

Figs. 9a, b show further comparisons, this time between the predicted and the measured horizontal components of force transmitted to ground, as measured by strain gauges fixed to the flexible bars 6 of the rig (Fig. 7). The same trends can be seen in both, the one exception being the continuous fairly steep rise in transmitted force with speed for the largest unbalance (1.9 gr-m) in Fig 9b. Fig.10a shows a predicted waterfall diagram which illustrates vibration occurring at engine-orders half, one and two. These engine orders are encouraged by such factors as transients or slight eccentricity from the centre of the squeeze-film damper. The rig's natural frequency component at 33Hz is however present at all rotor speeds, and, in particular, is excited by the half-order when the rotor speed is 66 rev/min. The jump-down in the 1EO is clearly discernible and coincides with the disappearance of the 2EO. As such it agrees with the experimental observations illustrated in Fig. 2c.

Finally, Fig. 10b shows an experimental waterfall diagram, for comparison with Fig.10a. Common features can be clearly seen, such as the strong first engine order, the ½EO exciting the natural frequency of 33 Hz at a rotor speed of 66 Hz and the 2EO, with its disappearance after the jump in the 1EO. Owing to the scale adopted to bring out the ½EO and 2EO, the 1EO was everywhere extremely large, but the jump certainly occurred at about 48 Hz as can be verified from Fig. 9b. The response at 84 Hz illustrates another natural frequency of the experimental rig which was not catered for in the theoretical model .

CONCLUSIONS

This paper has considered the case of a flexibly supported three-bearing rigid rotor utilising a squeeze-film damper at one of its bearings. It has shown that the assembly can be regarded for analysis as a parallel combination of spring and non-linear damper supporting the rotor mass. As a result, subharmonic resonances and jump phenomena are predicted.

A test facility has been described, which displays such phenomena and these have been presented in the form of response curves and a waterfall diagram. The frequency content in these shows close resemblance to theoretical predictions presented in the same form.

Finally, a relationship has been established between the linear stiffness and damping coefficients of a rotating-journal bearing for perturbation from an equilibrium position and the corresponding coefficients of a non-rotating squeeze-film damper for perturbation from an equilibrium orbit.

REFERENCES

[1]   HOLMES, R.   "The control of engine vibration using squeeze-film dampers".
       Trans ASME Journal of Engineering for Power July 1983 Vol 105 pp 525-529.

[2]   MOHAN, S and HAHN, E.J.   "Design of Squeeze film damper supports for rigid
       rotors" Trans. ASME Journal of Engineering for Industry Aug. 1974 pp 976-982.

[3]   NIKOLAJSEN, J.L. and HOLMES, R.   "Investigation of squeeze-film isolators for
       the vibration control of a flexible rotor" Jnl.Mech.Eng.Sci. Vol.21 No.4 1979
       pp 247-252.

[4] SIMANDIRI, S. and HAHN, E.J. "Experimental evaluation of the predicted behaviour of squeeze-film bearing supported rigid rotors". Jnl. Mech. Eng.Sci. Vol.21 No. 6 1979 pp 439-457,

[5] HOLMES, R. and DOGAN,M. "Investigation of a rotor-bearing assembly incorporating a squeeze-film damper bearing" Jnl. Mech. Eng.Sci. Vol.24 No. 3 1982 pp 129-137.

[6] PINKUS, O and STERNLIGHT, B. "Theory of hydrodynamic lubrication 1961, 267 (McGraw-Hill, New York).

[7] HOLMES, R. "Instability phenomena due to circular bearing oil-films". Jnl.Mech.Eng.Sci. Vol.8, No. 4, 1966, pp419-425.

a)

b)
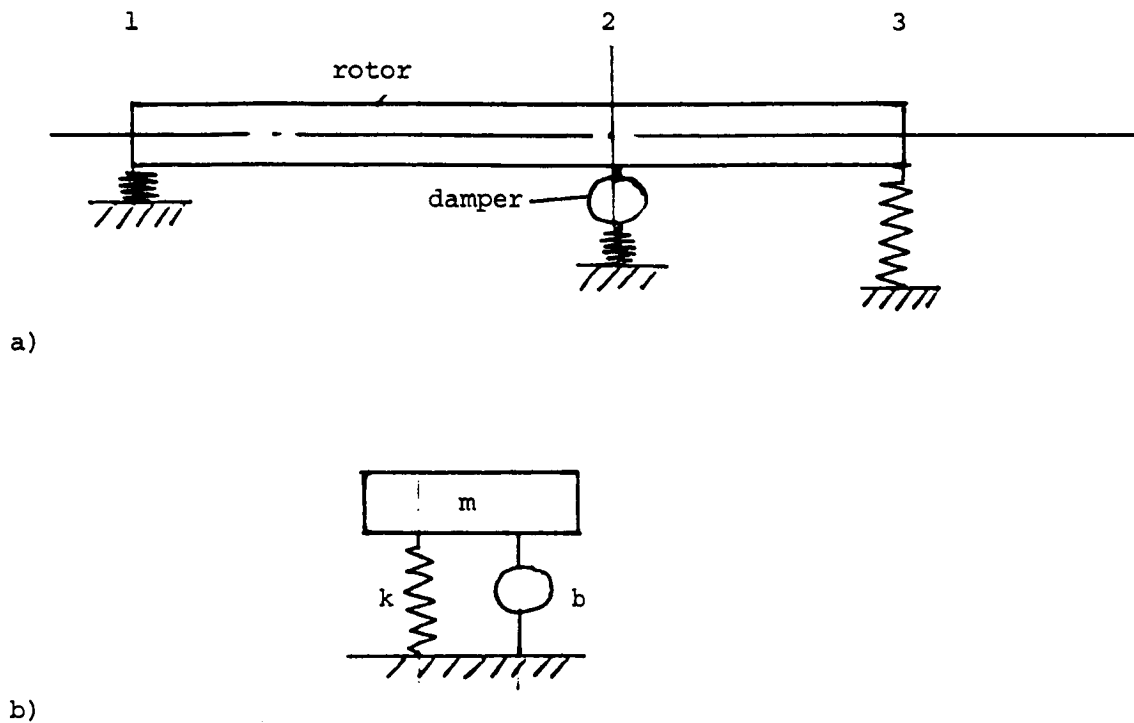
Figure 1. - Rotor and equivalent system.
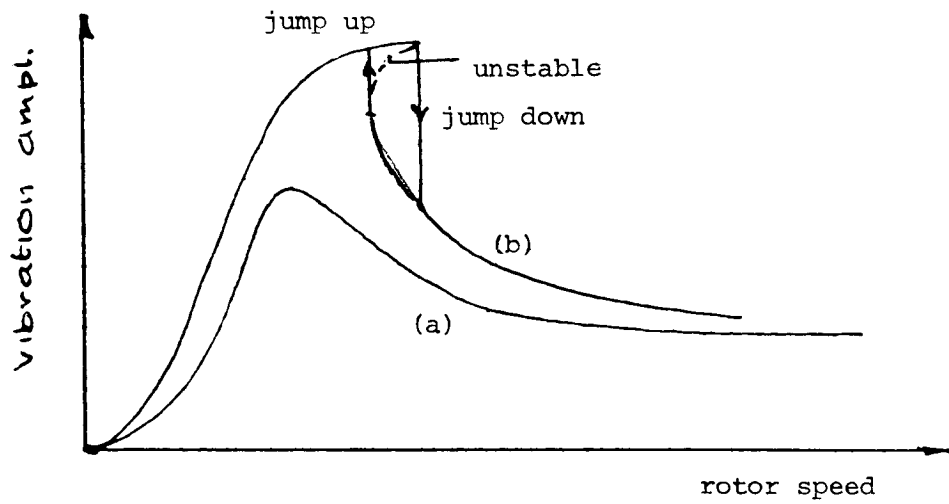
(a) Uncavitated rotor vibration response curve.
(b) Cavitated rotor vibration response curve.
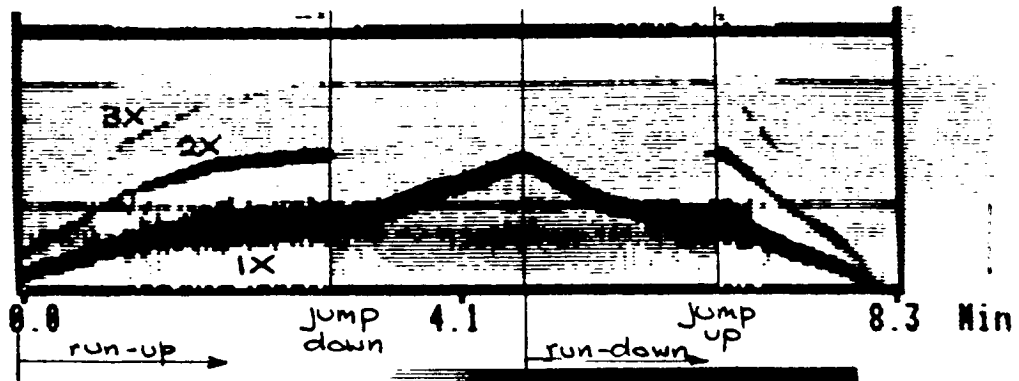
(c) Frequency diagram.
Figure 2. - Response curves and frequency diagram.
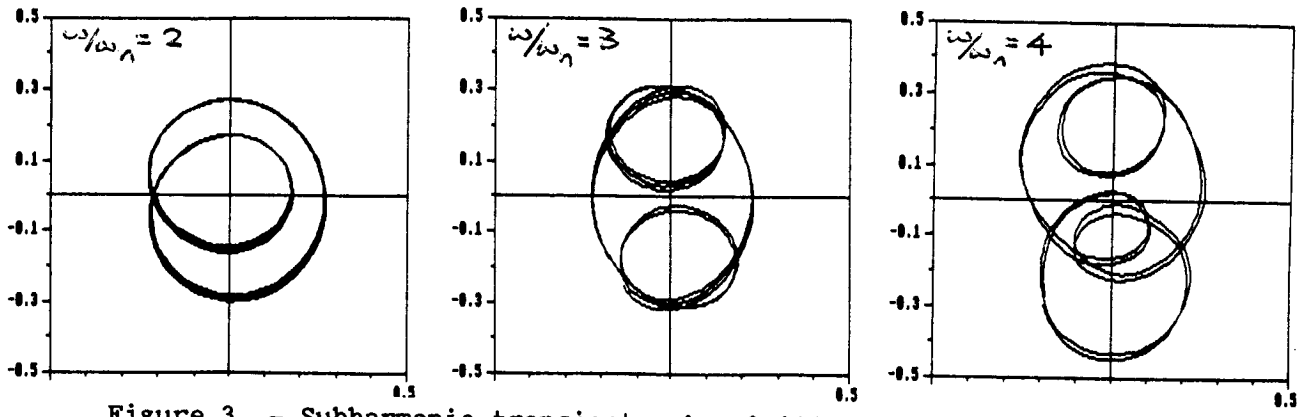
Figure 3. – Subharmonic transients; A = 0.014, u/c = 0.091; π film.
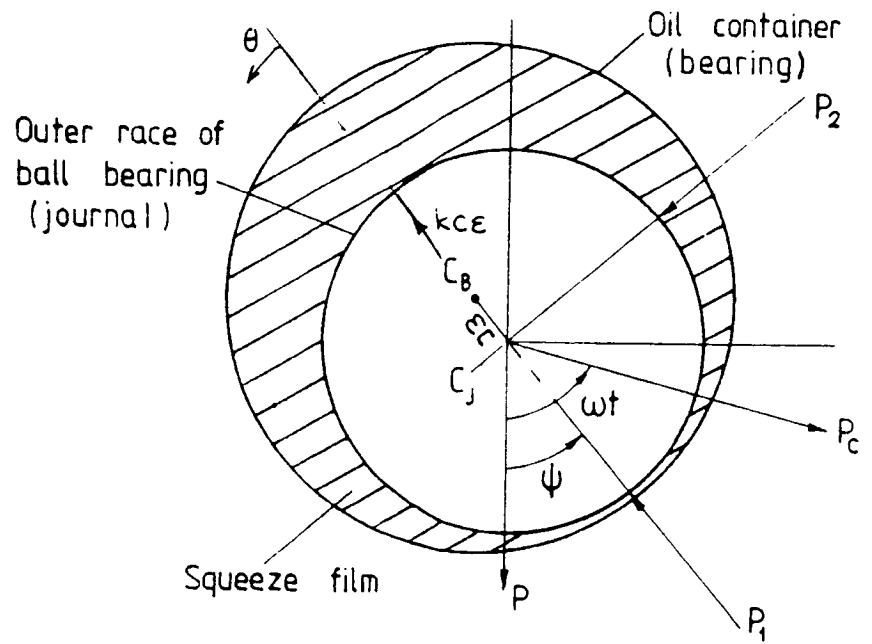
Figure 4. – Damper assembly.
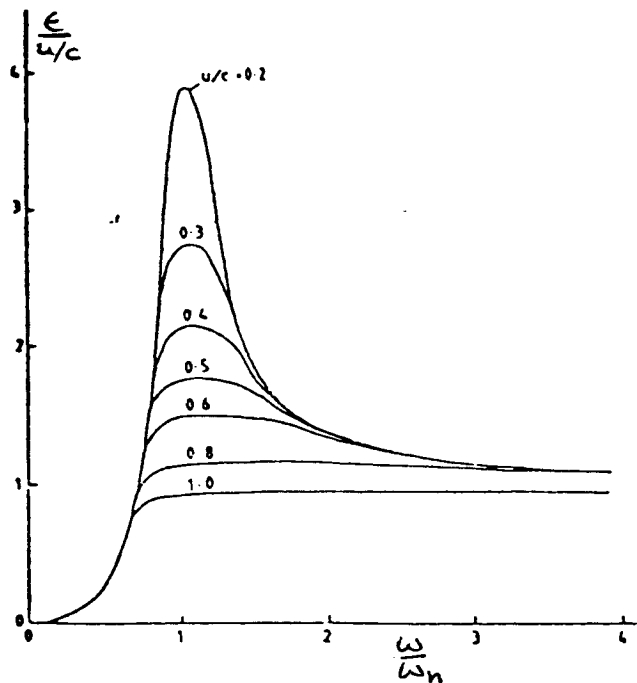
(a) Full-film frequency response.
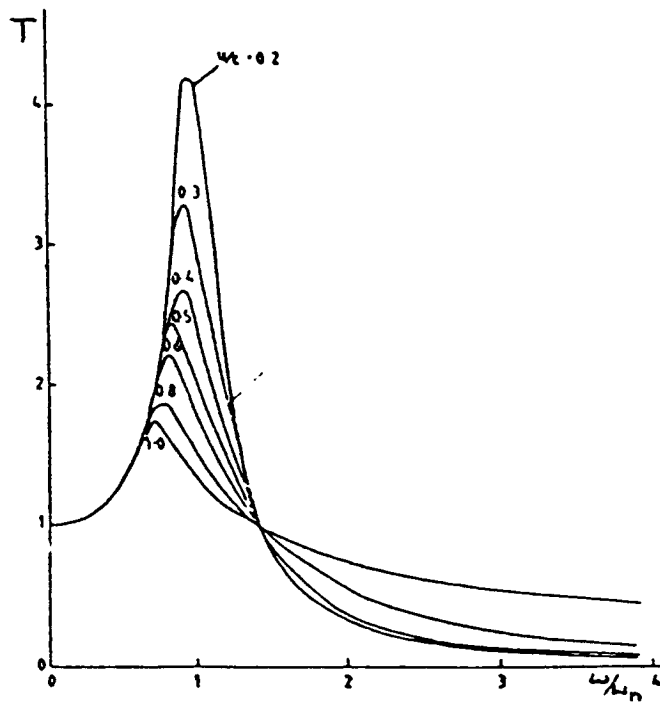
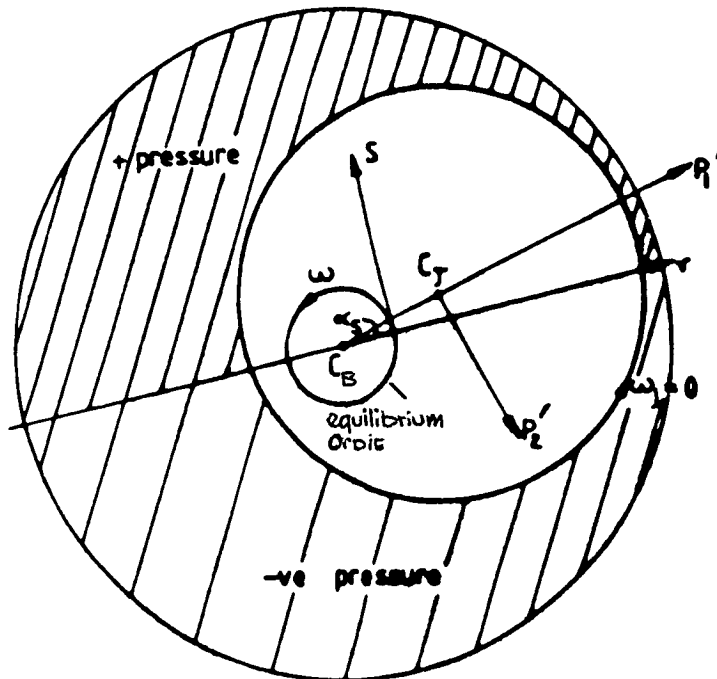(b) Full-film transmissibility.
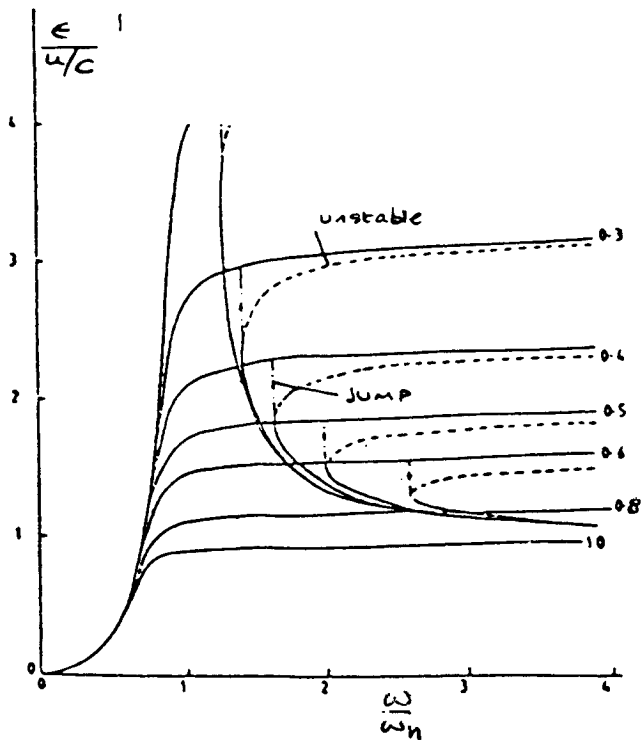
(c) Half-film frequency response.
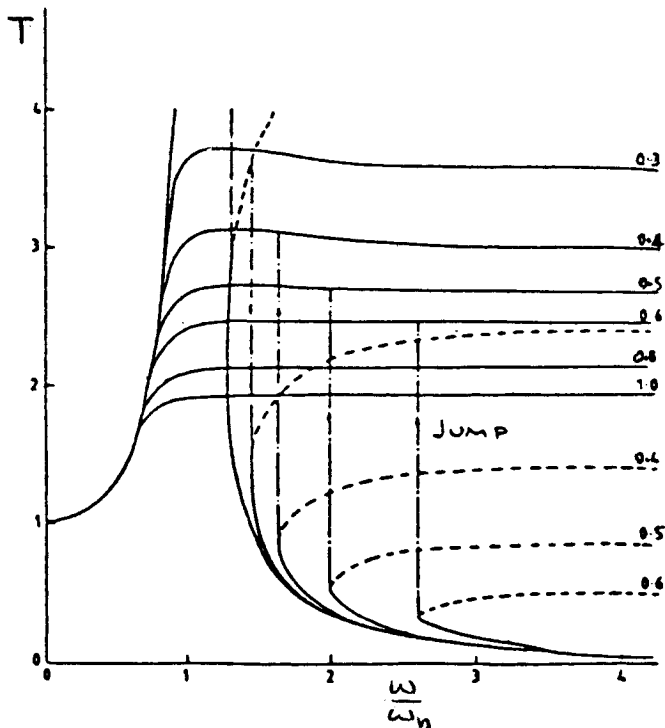
(d) Half-film transmissibility.
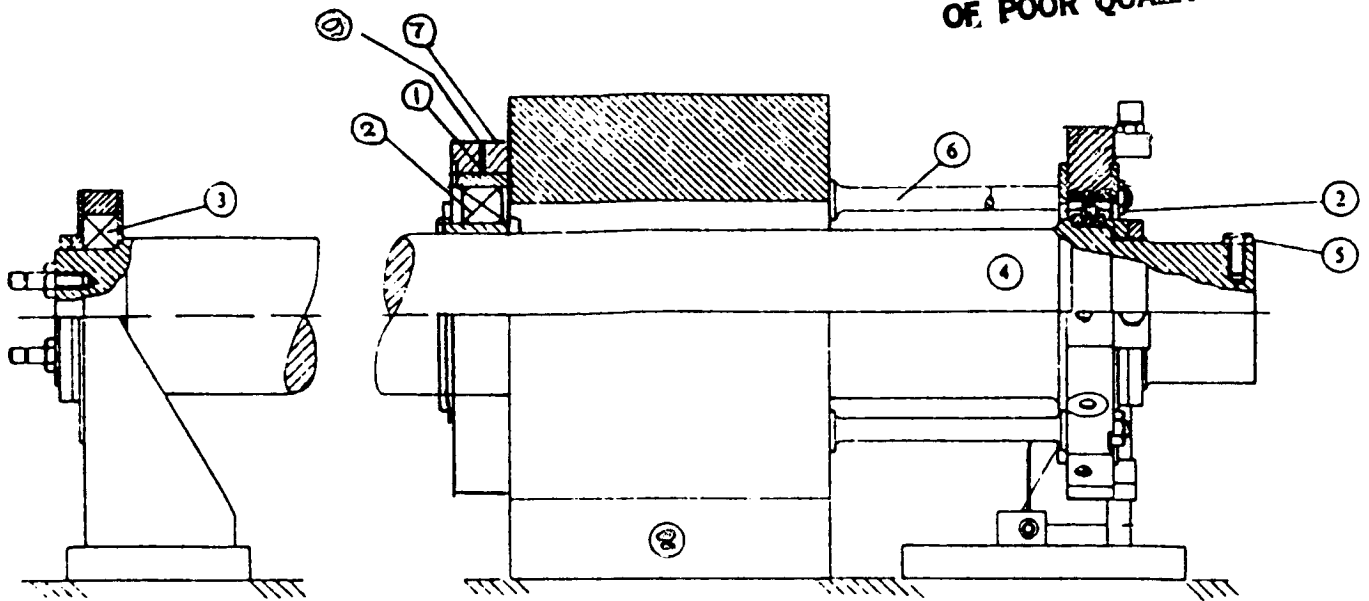
Figure 5. - Response curves.
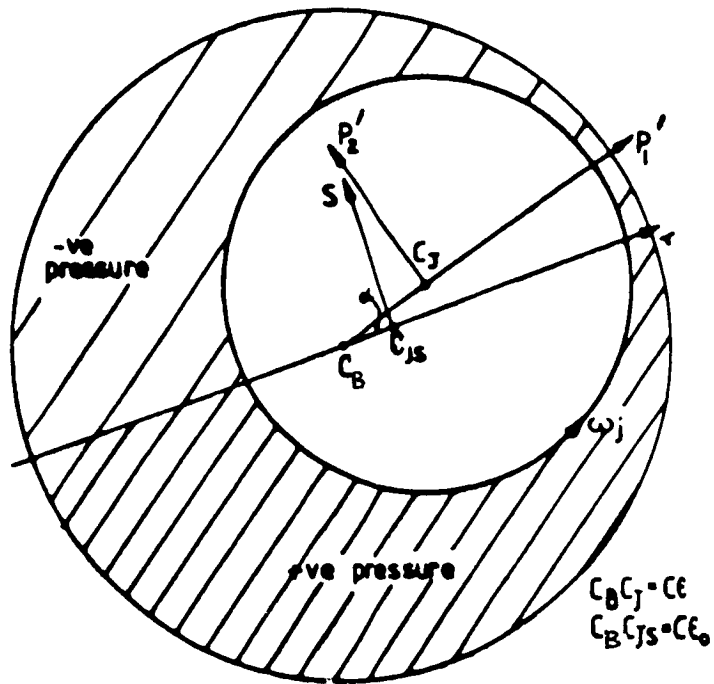
(a) Journal bearing; r and s are
stationary coordinates.

(b) Squeeze-film damper; r and s are
rotating coordinates.

Figure 6. – Comparison of journal bearing
with squeeze-film damper.

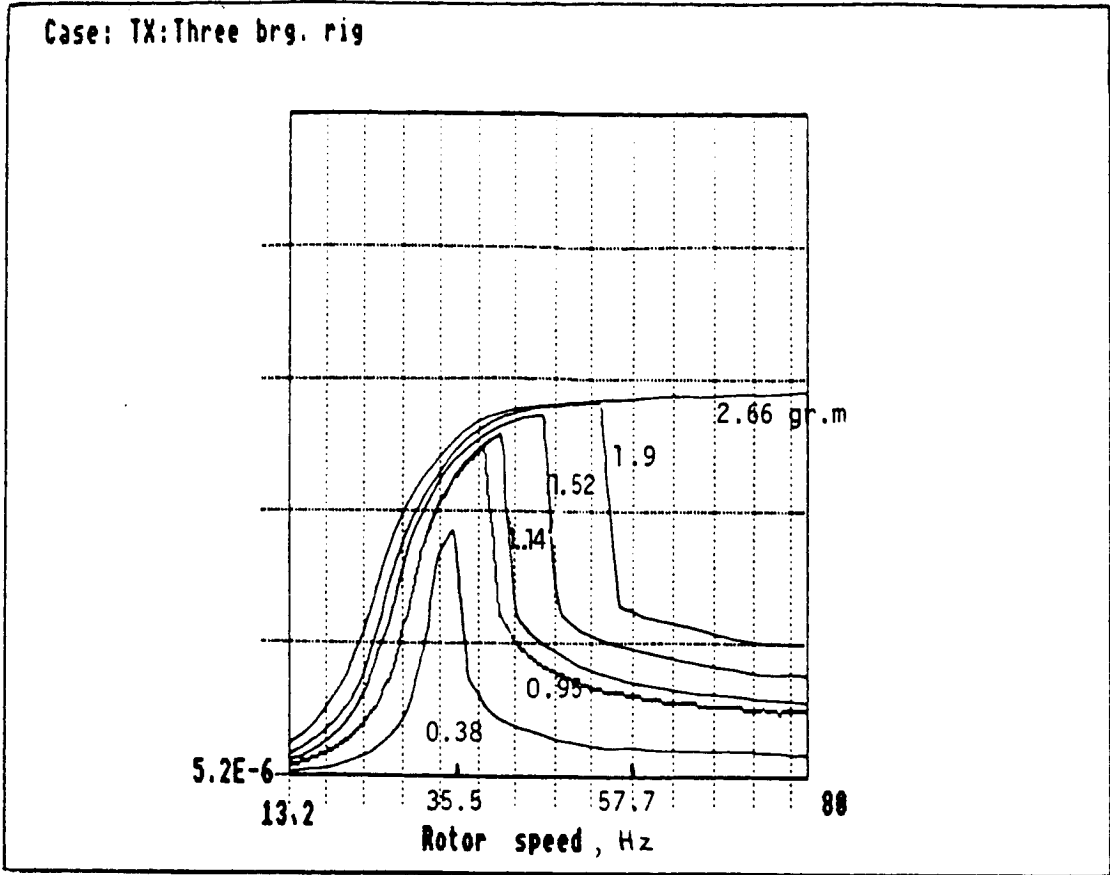|	
1 Squeeze-film damper	6 Flexible bars
2 Rolling element bearings	7 Housings
3 Self-aligning bearing	
4 Rotor	8 Foundation block
5 Unbalance mass	9 Oil supply

Figure 7. – Experimental rig.
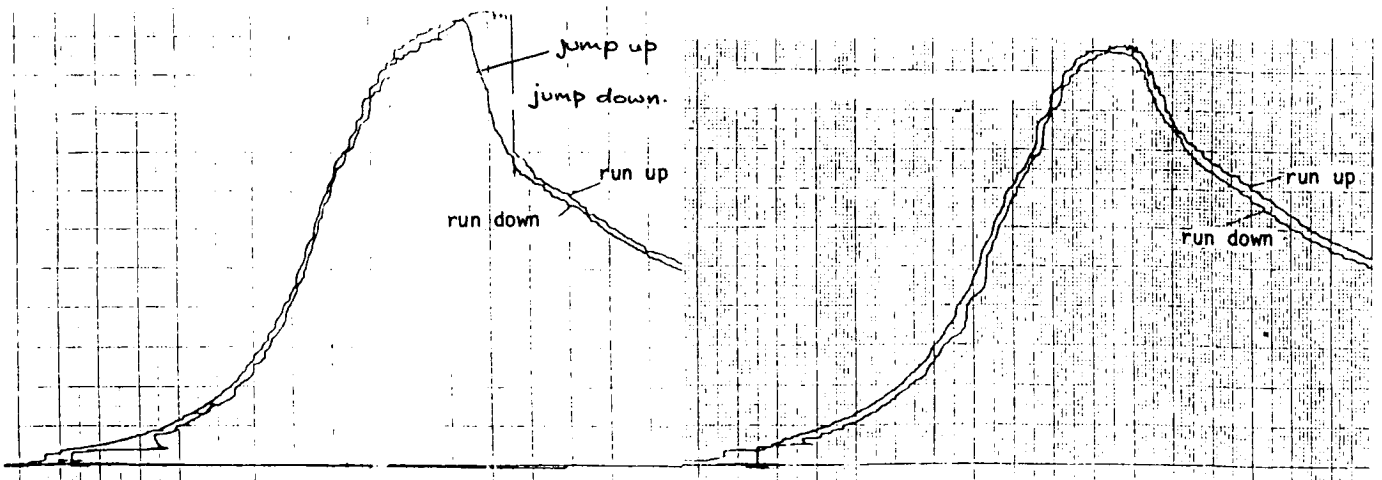
(a) Supply pressure, 2 lbf/in^2.   (b) Supply pressure, 10 lbf/in^2.
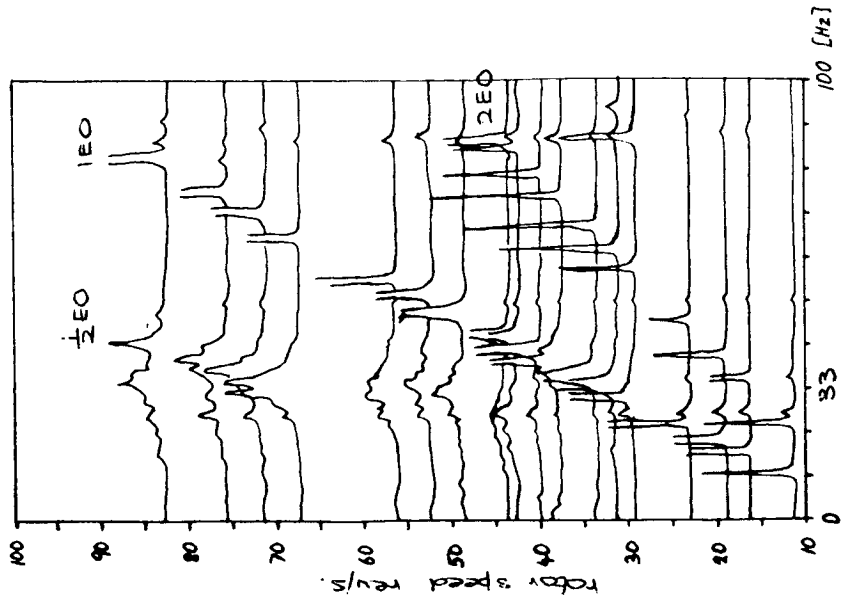
Figure 8. – Responses.

Case: TX:Three brg. rig

2.66 gr.m
1.9
1.52
1.14
0.95
0.38
5.2E-6
13.2   35.5   57.7   88
Rotor speed, Hz

(a) Predicted responses.

1.9 gr.m.
1.52
1.14
0.95

48   rotor speed, Hz
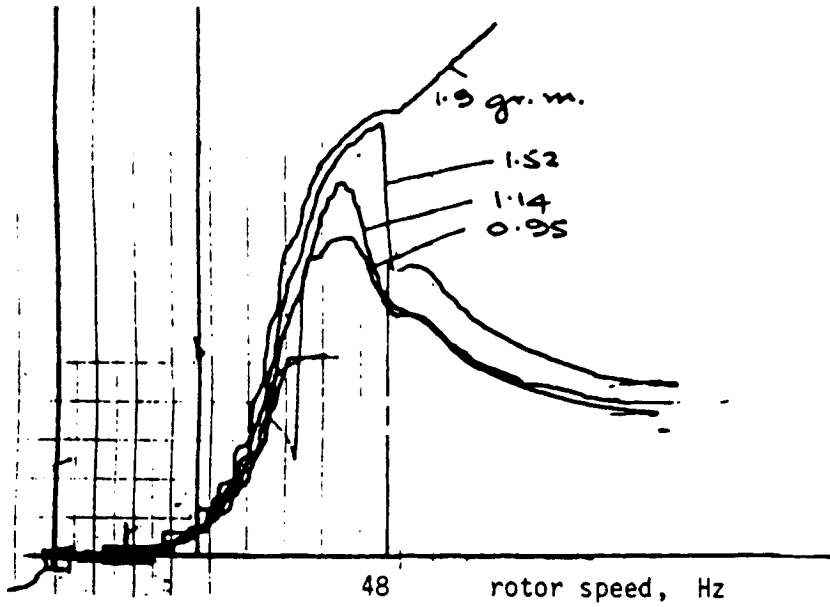
(b) Measured responses.

Figure 9. - Horizontal components of force transmitted to ground.

Case: TX:Three brg. rig:30gr:Ecc=0.25

(a) Predicted.
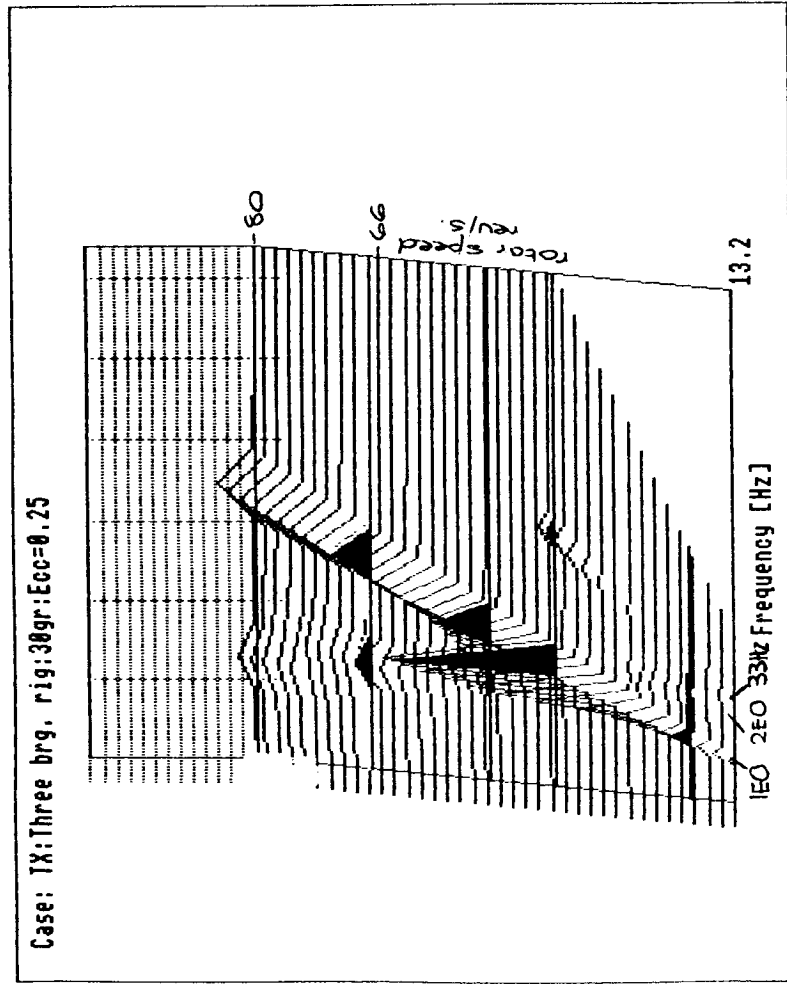
(b) Experimental.

Figure 10. - Waterfall diagram.

364